

## Infrared and Optical Spectroscopy of $\alpha$ - and $\gamma$ -Phase Cerium

J. W. van der Eb, A. B. Kuz'menko,\* and D. van der Marel

Material Science Center, University of Groningen, Nijenborgh 4, 9747 AG Groningen, The Netherlands  
(Received 10 October 2000)

We determined the optical properties of  $\alpha$ - and  $\gamma$ -phase Ce in the photon energy range from 60 meV to 2.5 eV using ellipsometry and grazing incidence reflectometry. We observe significant changes of the optical conductivity, the dynamical scattering rate, and the effective mass between  $\alpha$ - and  $\gamma$ -cerium. The  $\alpha$ -phase is characterized by a Fermi-liquid frequency-dependent scattering rate, and an effective mass of about  $20m_e$  on an energy scale of about 0.2 eV. In  $\gamma$ -Ce the charge carriers have a large scattering rate in the far infrared and a carrier mass characteristic of  $5d$  band electrons. In addition, we observe a prominent absorption feature in  $\alpha$ -Ce, which is absent in  $\gamma$ -Ce.

DOI: 10.1103/PhysRevLett.86.3407

PACS numbers: 78.20.-e, 71.27.+a, 71.28.+d, 75.30.Mb

One of the most intriguing phenomenon of cerium is the isostructural phase transition between a low temperature  $\alpha$ -phase and a high temperature  $\gamma$ -phase, which ends in a solid-solid critical point, where the two phases are indistinguishable. The structure is fcc with one atom per unit cell. It has become clear that the proximity of the  $4f$  level to the Fermi level is at the heart of these phenomena [1]. Recently the nature of the  $\gamma$ - $\alpha$  phase transition has been questioned by Eliashberg and Capellmann [2]. They argued that a second order phase transition line continues beyond the tricritical point on the melting curve, implying that the symmetries of the two phases are different. The question is which symmetry breaking takes place through the phase transition. Crystallographically the two phases appear to be identical [3]. Alternatively  $\alpha$ - and  $\gamma$ -Ce may correspond to states of matter with the same crystallographic symmetries, but with a "hidden" electronic symmetry which is broken in the  $\alpha$ -phase. This motivated us to embark on a series of spectroscopic experiments on the electronic structure [4] including the work presented here. Although we cannot argue on the basis of these experiments that a symmetry is broken, we do provide compelling evidence that the electronic structure of both phases is qualitatively different.

Although an extensive literature exists on optical properties of heavy fermion compounds, many of which are intermetallic compounds based on Ce [5], little is known about the optical spectra of pure metallic cerium [6–8]. Wilkins *et al.* reported several absorption peaks (288, 218, 170, 150, 83 meV) [6], which we have not been able to reproduce. Rhee *et al.* reported optical spectra from 1.5 to 5 eV on different films [8], with a large sample dependence of the data, and which were distinctly different from ellipsometry measurements of polycrystalline samples by Knyazev *et al.* [7].

In this Letter we present infrared/optical data over a broad range of photon energy. Using *in situ* thin film deposition technology we obtained excellent sample-to-sample reproducibility of the optical spectra.

Cerium is a highly reactive metal. In order to prepare and maintain a clean and oxygen-free sample over a period of about one day, it is necessary to work under ultrahigh vacuum (UHV). We used a compact UHV cryostat for low temperature *in situ* evaporation of Ce films, with vacuum in the  $10^{-10}$  mbar range. The ZnSe windows are transparent from 0.06 to 2.5 eV photon energy. Following the procedure outlined in Ref. [9] we prepared thin films of  $\alpha$ - and  $\gamma$ -phase Ce on clean and oxygen-free silicon wafers using ultrahigh vacuum deposition. The evolution of the optical spectra was monitored during the deposition process. The growth rate of about  $2 \text{ \AA/s}$  provided smooth mirrorlike films, in agreement with earlier reports [9], with optical properties which were reproducible over four cycles of deposition and measurement. Details of the sample preparation are given in Ref. [4].

For photon energies between 0.8 and 2.5 eV we measured the optical constants by using spectroscopic ellipsometry using an angle of incidence  $\theta$  of  $80^\circ$ . Ellipsometry provides directly the amplitude ratio ( $\tan\psi = |r_p/r_s|$ ) and phase difference [ $\Delta = \arg(r_p) - \arg(r_s)$ ] of the reflection coefficients ( $r_p$  and  $r_s$ ) of  $p$ - and  $s$ -polarized light, the dependence of which on the dielectric function,  $\epsilon(\omega)$ , is given by the ellipsometric formula,

$$\tan\psi e^{i\Delta} = \frac{\sin^2\theta - \cos\theta\sqrt{\epsilon - \sin^2\theta}}{\sin^2\theta + \cos\theta\sqrt{\epsilon - \sin^2\theta}}. \quad (1)$$

In the photon energy range of 60 meV to 0.8 eV we used a Fourier transform infrared spectrometer to measure the intensity ratio of the reflectivity coefficients of  $p$ - and  $s$ -polarized light, providing only  $\psi(\omega)$ , but not  $\Delta(\omega)$ . The conventional approach for obtaining  $\Delta(\omega)$  would be to use Kramers-Kronig relations between phase and amplitude. However, knowledge of the amplitude over only a limited frequency range is, in principle, insufficient to determine the phase function. As was shown in Refs. [10,11] a minimum of two "anchors" (frequencies where amplitude and phase have been measured) suffices to nail down the

phase in the entire frequency range where the amplitudes have been measured. In the present case we have anchored the phases from 0.8 to 2.5 eV, which allows us to determine the  $\Delta(\omega)$  between 0.06 and 0.8 eV in a very accurate way. Special care is needed here, because for  $\theta > 45^\circ$  the function  $\ln[\tan \psi(\omega)] + i\Delta(\omega)$  does not have all its poles in the lower half of the complex frequency plane, as can be verified easily from Eq. (1). On the other hand,  $\text{Re}\epsilon(\omega)$  and  $\text{Im}\epsilon(\omega)$  do satisfy this condition, implying that  $\epsilon(\omega)$  can always be represented as a sum of oscillators  $\epsilon(\omega) = 1 + \sum_j \omega_{pj}^2 \{\omega_{0j}^2 - \omega^2 - i\gamma_j \omega\}^{-1}$ . This means that any experimental  $\psi(\omega)$  and/or  $\Delta(\omega)$  spectrum can be fitted by adjusting the number of oscillators such as to reproduce all the details of the spectrum other than statistical noise. No obvious physical interpretation of the individual oscillators necessarily exists, as the oscillator sum is rather similar in nature to a Kramers-Kronig integral. By using Eq. (1), we determined  $\Delta(\omega)$  for  $\hbar\omega < 0.8$  eV with this analysis, using on input the experimental  $\psi(\omega)$  for  $0.06 < \hbar\omega < 2.5$  eV, and  $\Delta(\omega)$  for  $\hbar\omega > 0.8$  eV (see bottom panel of Fig. 1). The final step is to calculate  $\text{Re}\epsilon(\omega)$  and  $\text{Re}\sigma(\omega) = \omega \text{Im}\epsilon(\omega)/4\pi$  from the ellipsometric parameters using Eq. (1). For  $\omega > 0.8$  eV, we used the directly measured  $\psi$  and  $\Delta$ . For  $\omega < 0.8$  we used the directly measured  $\psi(\omega)$ , while  $\Delta(\omega)$  was determined with the analysis described above.

Following the analysis of Ref. [9] we identify the films deposited at temperatures below 4 K and above 300 K ( $\sim 400$  K in our case) as  $\alpha$ - and  $\gamma$ -phase Ce, respectively. We observed strong hysteresis of the optical spectra during cycling of the temperature after deposition. Similar hysteresis loops have been reported for the dc resistivity of Ce films by Löffler *et al.* [12]. In Fig. 1 we show  $\text{Re}\epsilon(\omega)$  and  $\text{Re}\sigma(\omega)$  for the  $\alpha$ - and the  $\gamma$ -phase. In the  $\alpha$ -phase the Drude contribution narrows and increases in intensity, leading to a more metallic behavior as expected.

At the lowest frequencies of our experiment the conductivity of  $\alpha$ -phase cerium is higher than that of the  $\gamma$ -phase, in qualitative agreement with the trends observed in the dc transport properties [12]. In addition to a very sharp Drude peak, we observe in  $\alpha$ -Ce a shoulder at 0.3–0.4 eV, and a peak at 1.0 eV, on top of a broad and featureless background conductivity. In the  $\gamma$ -phase the Drude peak is much broader, the shoulder is absent, and again there is a broad and almost featureless background, except for a weak and broad shoulder from 0.5 to 1.5 eV. The most significant difference is the presence of a prominent peak at 1 eV in the  $\alpha$ -phase, and the absence thereof in the  $\gamma$ -phase, indicating that the electronic structure of both phases is significantly different on an energy scale far exceeding the reported values of the Kondo temperature. The intensity and sharpness of this peak suggests that this is a virtual bound state of  $5d \rightarrow 4f$  character.

Cerium has four valence electrons per unit cell. One of the key issues is how these electrons are distributed between the quasiatomic  $4f$  states and the non- $4f$  conduc-

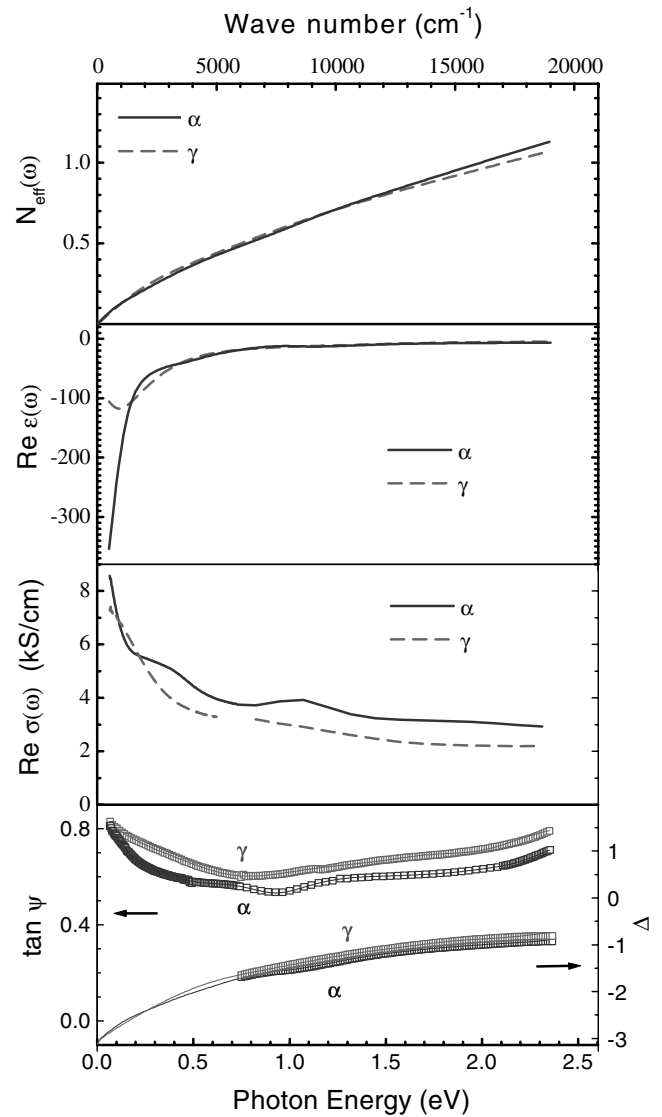


FIG. 1.  $\psi(\omega)$  and  $\Delta(\omega)$ . Open symbols: measured data. The solid curves are calculated by using the analysis explained in the text, and they overlap exactly with the symbols. Real part of the optical conductivity (second panel from below), real part of the dielectric constant (third panel from below), and spectral weight function (top panel) of  $\alpha$ - and  $\gamma$ -Ce.

tion bands (mainly  $5d$ ), and to what extent this distribution changes as a function of temperature. A powerful tool to address these issues is provided by an analysis of the spectral weight. In the top panel of Fig. 1 we display the function

$$N_{\text{eff}}(\omega) = \frac{2m_e \Omega_u}{\pi e^2} \int_0^\omega \sigma(\omega') d\omega', \quad (2)$$

where we used  $\Omega_u = 29.2 \text{ \AA}^3$  for the unit cell volume of  $\alpha$ -Ce and  $\Omega_u = 34.4 \text{ \AA}^3$  for  $\gamma$ -Ce. According to the  $f$ -sum rule the limiting behavior at high frequencies  $N_{\text{eff}}(\omega)$  reflects the *total* number of electrons (core and valence). If the integration is restricted to the Drude peak,

$N_{\text{eff}}(\omega)$  corresponds to the  $k$ -space (Luttinger) volume occupied by the valence electrons, multiplied by  $m_e/m_b$ , where  $m_b$  is the band mass of the conduction electrons. For both phases,  $N_{\text{eff}}(\omega) \sim 1$  between 1.5 and 2.5 eV. However, even at 2.5 eV there is no saturation of  $N_{\text{eff}}(\omega)$ . This implies that interband transitions and electron-electron scattering processes continue to contribute to the optical absorption in the ultraviolet. An upper limit of  $m_b$  can be set to  $\sim 6m_e$ , which is reasonable given the fact that these bands have mainly  $5d$  character [13,14].

Let us consider the case of  $\alpha$ -cerium at low frequencies, and let us assume at this point that the narrow Drude peak below  $\sim 0.2$  eV is the response of all four valence electrons, with the same effective mass. To estimate the spectral weight of the narrow peak, we chose  $\omega \approx 0.2$  eV as the upper limit of integration. Because  $N_{\text{eff}}(0.2 \text{ eV}) \approx 0.2$ , this implies that close to  $E_F$  the valence electrons have an effective mass  $m^*/m_e \approx 20$ . In reality the Fermi surface has a complicated shape, and the mass may have a strong  $k$  dependence along the various sections of this Fermi surface. As a consequence  $m^*$  should be regarded as a quantity representing the *average* effective mass.

Let us now consider the  $\gamma$ -phase. In this case we have good reason to make a clean distinction between the localized  $4f$  states and the conduction bands of mainly  $5d$  character. Because of their localized character, the  $4f$  electrons have a negligible contribution to the low frequency spectral weight. As a result the Drude peak extending up to about 1 eV is mainly of  $5d$  character, and three electrons contribute to the Drude peak. Reading  $N_{\text{eff}}(0.6 \text{ eV}) \approx 0.5$  for the  $\gamma$ -phase, we conclude that the effective mass of the conduction electrons of  $\gamma$ -Ce is about  $\sim 6m_e$ .

Another way to analyze the nature of the low frequency spectral weight is to calculate the frequency-dependent effective mass  $m^*(\omega)$  and scattering rate  $1/\tau(\omega)$  directly from the real and imaginary part of the optical conductivity, using the generalized Drude form [15]

$$\sigma(\omega) = \frac{ne^2/m_e}{\tau(\omega)^{-1} + i\omega m^*(\omega)/m_e} \quad (3)$$

and using  $n = 4/\Omega_u$  for the density of valence electrons. The results are shown in Fig. 2. The large mass enhancement in the  $\alpha$ -phase indicates that the valence bands at the Fermi energy are strongly renormalized. The heavy mass indicates that at least one of the bands crossing the Fermi has considerable  $4f$  character and/or a strong mass renormalization due to coupling to spin fluctuations. The width of the effective mass peak is about 0.2 eV, which indicates that coherent Bloch-like states exist below a typical energy scale  $k_B T_{\text{coh}} = 0.2$  eV [16]. At higher energies the Fermi-liquid type mass renormalization reduces gradually to the mass of a bare band electron, and in Fig. 2 we see that the effective mass of the  $\alpha$ -phase approaches that of the  $\gamma$ -phase above 0.6 eV. The frequency-dependent scattering rate of the  $\alpha$ -phase bears a strong resemblance to

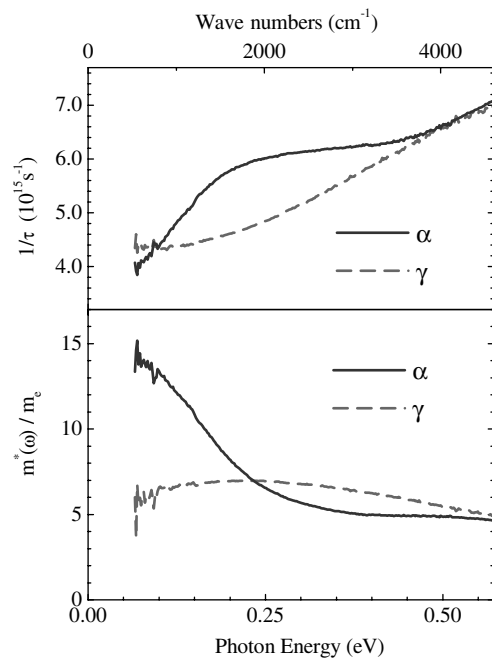


FIG. 2. Frequency-dependent effective mass (bottom panel) and scattering rate (top panel) of  $\alpha$ - and  $\gamma$ -Ce.

Fig. 13.3 of Ref. [16], which, in the context of the Kondo lattice model, indicates that a narrow band of itinerant electrons is formed with a coherence temperature  $k_B T_{\text{coh}} = 0.2$  eV, and a characteristic heavy-fermion temperature  $k_B T^* = 0.4$  eV.

The frequency dependence of the scattering rate and effective mass of  $\alpha$ -Ce has similar characteristics as the heavy-fermion compound  $\text{URu}_2\text{Si}_2$ , for which  $k_B T_{\text{coh}} = 6$  meV and a mass enhancement factor of 50 has been reported [17]. The frequency dependence  $1/\tau$  and  $m^*$  (Fig. 2) are directly visible as a shoulder at 0.3 eV in the conductivity of  $\alpha$ -Ce (Fig. 1). The spectra of  $\alpha$ - and  $\gamma$ -Ce agree very well with calculations based on the local impurity self-consistent approximation of the Anderson model by Rozenberg, Kotliar, and Kajueter (Fig. 20 of Ref. [18]) for temperatures far below ( $\alpha$ -Ce) and above ( $\gamma$ -Ce)  $T^*$ . Similar sidebands have been observed in  $\text{UPd}_2\text{Al}_3$  (1 meV [19]),  $\text{UPt}_3$  (1 meV [20]),  $\text{CeCu}_6$  (5 meV [21]),  $\text{UNi}_2\text{Al}_3$  (25 meV [22]), and  $\text{Yb}_{1-x}\text{Lu}_x\text{B}_{12}$  [ $(1-x) \cdot 0.25$  eV [23]]. It is conceivable that at least for some of these other materials the sideband is of a similar nature as in  $\alpha$ -Ce. The large variation of the position of the sideband among the different heavy-fermion systems would then reflect a variation of the coherence temperature from system to system, which is a lower energy scale than the on-site electron-electron interactions (Hubbard  $U$ ) [18]. The hierarchy of energy scales in heavy-fermion systems is believed to be  $T_{\text{coh}} \leq T^* \leq T_K$ , providing indirect evidence that  $T_K$  is several thousand K for  $\alpha$ -Ce, in agreement with the analysis of Allen and Martin [24]. They estimated that  $T_K$  of the  $\gamma$ -phase is of order 20 K

[24,25]. Under these conditions the mass renormalization effects are small. On the other hand, the partly filled  $4f^1$  states at each Ce atom still act as paramagnetic impurities, which form an efficient source for resonant scattering of the valence electrons. This is visible as a large residual scattering rate, as suggested by saturation of  $1/\tau(\omega)$  to a high value in the far-infrared range.

An interesting consequence emerges from these considerations:  $\gamma$ -Ce corresponds to a state of matter with three valence electrons per atom. The fourth electron contributes only a single spin degree of freedom, while the charge degree of freedom is gapped at an energy scale of several eV. The  $\alpha$ -phase, on the other hand, corresponds to a state where all four valence electrons participate in itinerant bands. This result has common factors with the Mott model of Johansson [26] and with the Kondo volume collapse (KVC) model [24,25]. The difference with the Mott model is that not four, but only one  $4f$  electron undergoes a Mott transition. With the KVC model it shares the property that the  $\gamma$ -phase consists of a band of itinerant electrons, weakly exchange coupled to paramagnetic local moments. The main difference is for the  $\alpha$ -phase, where our optical data suggest that an itinerant band is formed, a feature which requires explicit consideration of the lattice aspect of the problem. These aspects have been recently taken into account by Laegsgaard and Svane [27] in a model combining SIC-LDA and the Anderson impurity model. Is indeed a hidden electronic symmetry broken in the  $\alpha$ - $\gamma$  transition? The disappearance of one charge degree of freedom per atom as the system enters the  $\gamma$ -phase suggests that the answer to this question is affirmative.

We performed infrared grazing incidence measurements on cerium thin films. The conductivity shows a remarkable change between the  $\alpha$ - and  $\gamma$ -phases. A significant difference is the presence of a prominent peak at 1 eV in the  $\alpha$ -phase, and the absence thereof in the  $\gamma$ -phase, indicating that the electronic structure is significantly different in both phases on an energy scale far exceeding the reported values of the Kondo temperature of both phases. At low frequencies,  $\alpha$ -Ce is found to be reminiscent of a Fermi liquid with an effective mass of  $20m_e$ . We observe this behavior on an energy scale of about  $k_B T_{\text{coh}} = 0.2$  eV, above which  $\tau(\omega)^{-1}$  and  $m^*(\omega)$  saturate at  $6 \times 10^{15} \text{ s}^{-1}$  and  $5m_e$ , respectively. In the  $\gamma$ -phase the three conduction electrons have an effective mass of  $\sim 6m_e$ , with a large residual scattering rate ( $4 \times 10^{15} \text{ s}^{-1}$ ) in agreement with the notion of valence electrons resonantly scattered by  $4f^1$  local moments.

We thank G.M. Eliashberg for drawing our attention to this problem. A.B.K. was supported by the Russian Foundation of Basic Research, Grant No. 99-02-17752, and by the Nederlandse Organisatie voor Wetenschappelijk Onderzoek (NWO). This investigation was supported by the Netherlands Foundation for Fundamental Research on Matter (FOM) with financial aid from NWO.

*Note added.*—An explicit realization of a hidden electronic symmetry breaking has been recently proposed by Nikolaev and Michel [28].

\*Also at P.L. Kapitza Institute for Physical Problems RAS, Kosygina str. 2, Moscow, 117334, Russia.

- [1] For a recent review, see A.K. McMahan *et al.*, *J. Comput. Aided Mater. Des.* **5**, 131 (1998).
- [2] G.M. Eliashberg and H. Capellmann, *JETP Lett.* **67**, 125 (1998).
- [3] D.A. Koskenmaki and K.A. Gschneidner, in *Handbook on the Physics and Chemistry of Rare Earths*, edited by K.A. Gschneidner and L. Eyring (North-Holland, Amsterdam, 1978), Chap. 4.
- [4] J.W. van der Eb, Ph.D. thesis, University of Groningen, 2000.
- [5] L. Degiorgi, *Rev. Mod. Phys.* **71**, 687 (1999).
- [6] J.F. Wilkins, J.G. Clark, and T.E. Leinhardt, *Bull. Am. Phys. Soc.* **51**, 579 (1962).
- [7] Yu. V. Knyazev *et al.*, *J. Low Temp. Phys.* **17**, 1143 (1991) (translated from Russian).
- [8] J. Y. Rhee *et al.*, *Phys. Rev. B* **51**, 17 390 (1995).
- [9] E. Weschke *et al.*, *Phys. Rev. B* **44**, 8304 (1991); D. Wieliczka *et al.*, *Phys. Rev. B* **26**, 7056 (1982); F. Patthey *et al.*, *Phys. Rev. Lett.* **55**, 1518 (1985).
- [10] G. W. Milton, D. J. Eyre, and J. V. Mantese, *Phys. Rev. Lett.* **79**, 3062 (1997).
- [11] I. Bozovic, *Phys. Rev. B* **42**, 1969 (1990).
- [12] E. Löffler and J. A. Mydosh, *Solid State Commun.* **13**, 615 (1973).
- [13] W. E. Pickett, A. J. Freeman, and D. D. Koelling, *Phys. Rev. B* **23**, 1266 (1981).
- [14] A. B. Shick, W. E. Pickett, and A. I. Liechtenstein, *cond-mat/0001255*.
- [15] J. W. Allen and J. C. Mikkelsen, *Phys. Rev. B* **15**, 2952 (1977).
- [16] P. Fulde, in *Electron Correlations in Molecules and Solids* (Springer, Berlin, 1995), 3rd ed.
- [17] D. A. Bonn, J. D. Garrett, and T. Timusk, *Phys. Rev. Lett.* **61**, 1305 (1988).
- [18] M. J. Rozenberg, G. Kotliar, and H. Kajueter, *Phys. Rev. B* **54**, 8452 (1996).
- [19] M. Dressel *et al.*, *Physica (Amsterdam)* **244B**, 125 (1998).
- [20] G. Grüner, *Physica (Amsterdam)* **244B**, 70 (1998); P. E. Sulewski *et al.*, *Phys. Rev. B* **38**, 5338 (1988); F. Marabelli, P. Wachter, and J. J. M. Franse, *J. Magn. Magn. Mater.* **62**, 287 (1986); A. Awasthi *et al.*, *Phys. Rev. B* **39**, 2377 (1989).
- [21] F. Marabelli and P. Wachter, *Phys. Rev. B* **42**, 3307 (1990).
- [22] N. Cao *et al.*, *Phys. Rev. B* **53**, 2601 (1996).
- [23] H. Okamura *et al.*, *Phys. Rev. B* **62**, R13265 (2000).
- [24] J. W. Allen and R. Martin, *Phys. Rev. Lett.* **49**, 1106 (1982).
- [25] O. Gunnarsson and K. Schönhammer, *Phys. Rev. B* **28**, 4315 (1983); **31**, 4815 (1985).
- [26] B. Johansson, *Philos. Mag.* **30**, 469 (1974).
- [27] J. Laegsgaard and A. Svane, *Phys. Rev. B* **59**, 3450 (1999).
- [28] A. V. Nikolaev and K. H. Michel, *Eur. Phys. J. B* **17**, 363 (2000).